Dissolution dynamics of thin films measured by optical reflectance

Christian Punckt and Ilhan A. Aksay[a)]
Department of Chemical Engineering, Princeton University, Princeton, New Jersey 08544, USA

(Received 27 August 2009; accepted 2 December 2009; published online 29 December 2009)

Measuring the dissolution dynamics of thin films *in situ* both with spatial and temporal resolution can be a challenging task. Available methods such as scanning electrochemical microscopy rely on scanning the specimen and are intrinsically slow. We developed a characterization technique employing only an optical microscope, a digital charge coupled device camera, and a computer for image processing. It is capable of detecting dissolution rates of the order of nm/min and has a spatial and temporal resolution which is limited by the imaging and recording setup. We demonstrate the capabilities of our method by analyzing the electrochemical dissolution of copper thin films on gold substrates in a mild hydrochloric acid solution. Due to its simplicity, our technique can be implemented in any laboratory and can be applied to a variety of systems such as thin film sensors or passive coatings. © *2009 American Institute of Physics*. [doi:10.1063/1.3276631]

I. INTRODUCTION

Noninvasive, sensitive, and versatile experimental techniques for the spatiotemporally resolved measurement of corrosion rates of thin films are in high demand for the quantification of material degradation in microelectromechanical devices[1–3] or composite materials.[4–7] A variety of powerful *in situ* corrosion monitoring techniques has been developed or adapted for this purpose over the past decades, including scanning electrochemical microscopy (SECM) pioneered by Bard *et al.*,[8,9] scanning tunneling microscopy (STM),[10–13] and atomic force microscopy,[14,15] as well as optical techniques such as imaging ellipsometry,[16–19] holography,[20] interferometric microscopy (IM),[21,22] or confocal scanning laser microscopy.[23]

All these techniques offer a possibility to monitor the rate of dissolution or deposition of matter in an electrochemical (liquid) environment with spatial resolution. However, while for example SECM provides outstanding spatial resolution (as do most scanning methods) and accurate electrochemical data, the temporal resolution is low since a single image acquisition takes several minutes. Quantitative optical techniques either do not provide spatial resolution,[24] or require complicated instrumentation[21–23] and often lack temporal resolution.[18,19] The goal of this paper is to present a simple yet sensitive technique for the quantitative measurement of thin film dissolution and deposition in an arbitrary, optically transparent environment with the specific focus on monitoring a galvanic corrosion reaction.

In a recent study, we used a simple light reflection technique, developed in our laboratory, for the quantitative optical measurement of dissolution rates of galvanically corroding copper thin films based on bright field optical microscopy.[25] Here, we provide an in-depth analysis of this technique. In the following, we briefly discuss the theoretical background of our measurement principle focusing on metal thin films and present possible experimental settings. Using a simple model system consisting of copper islands on gold films, we demonstrate how our imaging system can be calibrated and used for *in situ* measurement of dissolution rates. Finally, we briefly compare our method with selected quantitative *in situ* techniques such as IM and scanning techniques.

Metal thin films with a thickness smaller than a tenth of the wavelength of visible light exhibit a considerable amount of optical transparency.[26] Figure 1(a) shows the calculated transparency, reflectivity, and absorption of a homogeneous metal thin film in air under illumination with monochromatic light of wavelength $\lambda=550$ nm at normal incidence as a function of the film thickness d. The complex refractive index $n=0.62+2.57i$ used in the calculation corresponds to that of bulk copper.[26] However, this gives only a qualitative estimate of the actual optical response of a copper film, since a thin film certainly does not exhibit bulk optical properties.

Up to a thickness of $d\approx 60$ nm, the film shows a monotonous decrease in transparency and a corresponding increase in reflectivity, which is observable with an optical microscope in transmission or reflection mode [Fig. 1(b)]. In fact, for $d<40$ nm, the reflectance appears to be a fairly linear function of film thickness. For $d>80$ nm, the optical properties asymptotically assume the properties of the bulk metal (saturation). Therefore, by measuring the reflection or transmission coefficient of a metal thin film with a thickness of a few tens of nanometers, we can—after proper calibration—quantitatively determine the film thickness.

This simple scenario becomes slightly more complicated if we consider a metal thin film on top of another (metallic) nontransparent substrate. Microscopic observation has now to be conducted in reflection mode, and instead of a transition from a nonreflective ($d=0$ nm) to a reflective ($d>0$ nm) state for increasing film thickness we observe a smooth transition from the reflective properties of the

[a)]Author to whom correspondence should be addressed. Tel.: (609) 258-4393. Electronic mail: iaksay@princeton.edu.

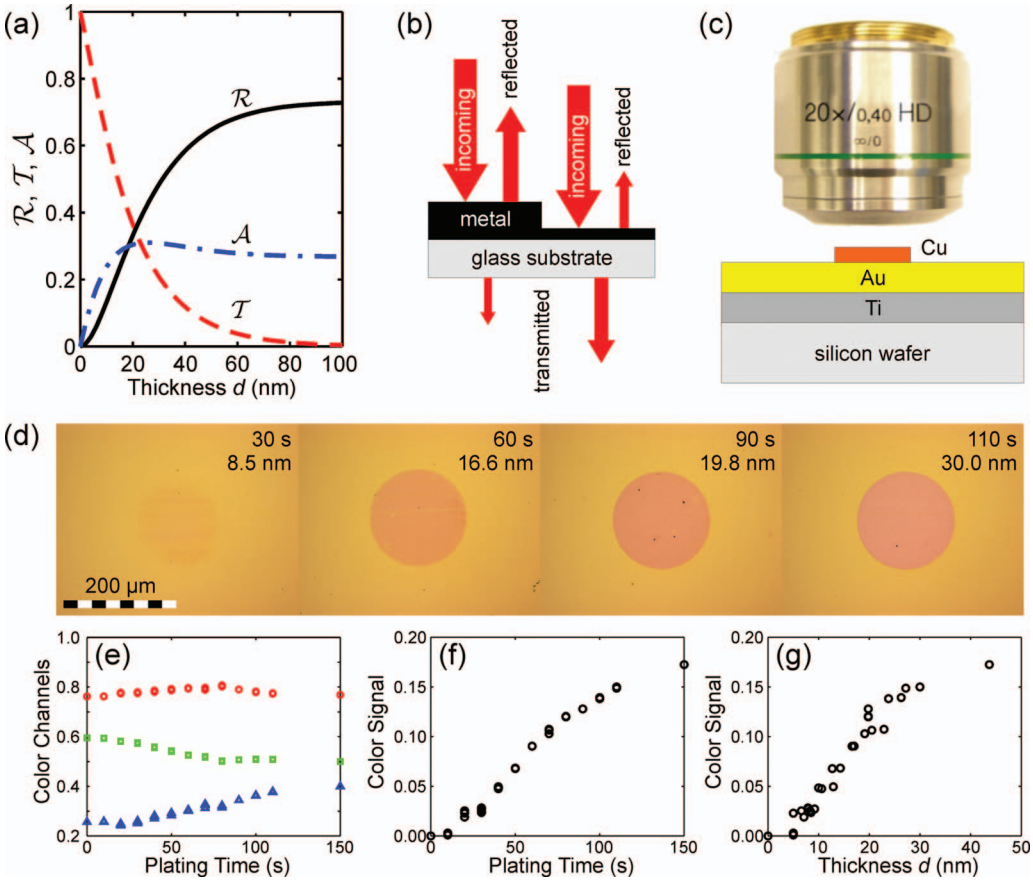

FIG. 1. (a) Calculated reflection (R), transmission (T), and absorption (A) coefficient of a copper thin film illuminated with monochromatic light with a wavelength of $\lambda = 550$ nm as a function of film thickness. (b) Possible measurement configurations. The thickness of a thin film on glass could be either determined in transmission or reflection since with increasing metal film thickness the transmissivity decreases while the reflectivity increases. (c) Calibration setup for measurement of copper islands in reflection. (d) Bright field microscopic images of copper disks on a gold substrate (thickness as indicated). (e) Color of copper islands in a recorded image such as shown in (d). The color is represented by the normalized average values of the three color channels red (circles), green (squares), and blue (triangles). [(f) and (g)] Average color signal (see text) as a function of plating time (e) and measured film thickness (f).

substrate to the reflective properties of the film until saturation is reached. Generally, we can no longer assume that reflectivity increases with increasing film thickness but instead more sophisticated measures need to be applied in order to perform a thickness calibration. In the following, we demonstrate how, based on a simple color analysis, we can determine the thickness of copper films on a gold substrate with nanometer accuracy.

II. EXPERIMENTAL

Samples for calibration measurements were prepared by evaporating 10 nm of titanium and 100 nm of gold on a silicon wafer using e-beam evaporation (Denton DV-502A, Denton Vacuum). The gold surfaces were coated with copper films of various thicknesses by electroless plating. After this, the copper films were patterned photolithographically and etched resulting in copper islands on a continuous gold background. The thickness of the final copper pattern was determined using a surface profiler (KLA-Tencor). With the optical microscope (Zeiss Axioplan 2, Carl Zeiss MicroImaging, Inc.), we recorded color images of copper islands of different thickness using white light illumination (halogen lamp) and a 12-bit digital charge coupled device (CCD) camera (Zeiss AxioCam HRc, Carl Zeiss MicroImaging, Inc.). Images were stored on a computer for further analysis with MATLAB™. A sketch of the imaging setup is displayed in Fig. 1(c).

III. RESULTS AND DISCUSSION

Figure 1(d) shows images of copper islands with thicknesses between 8.5 and 30 nm corresponding to plating times ranging from 30 to 110 s. From the digital images of our copper islands of various thicknesses, we extract color data for the thickness calibration in the following way. Our images are stored in an uncompressed bitmap file format (tagged image file format) with a color depth of 24 bits per pixel. The color of each pixel is described by three integer numbers with values between 0 and 255, representing the three color components red, green, and blue (RGB). Thus, after normalization, each pixel can be represented as a point in the three-dimensional unit cube (normalized color space). Figure 1(e) shows the color of different copper films in normalized RGB representation as a function of plating time.

Color differences between different locations (pixels) in one image or between subsequent snapshots of the same location can be expressed as the Euclidic distance between the

corresponding points in the normalized color space. We call the distance between the two corresponding points in the normalized color space "color signal." The average color of a specific copper structure can be determined by averaging over a large number of pixels in the copper area, and the same can be done for the gold substrate. From the average color of the gold and the copper surfaces of our calibration samples we calculate an average color signal for each copper island. These color signals are plotted as a function of plating time and measured thickness in Figs. 1(f) and 1(g). The larger noise observed in Fig. 1(g) as compared to Fig. 1(f) is probably due to statistical errors in the thickness measurement using the profiler.

As can be seen in Fig. 1(g), there is an approximately linear correlation between the thickness of the copper film and the color signal up to a thickness of about 30 nm (corresponding to a plating time of 110 s). This corresponds to our initial calculations for a thin metal film in air. With increasing thickness, the copper film becomes less transparent and optical properties of the underlying gold layer are superimposed by the properties of the copper film.

Caution has to be exercised when film thickness is calculated based on color data, since copper can form a native oxide or oxyhydroxide layer when exposed to humid air or aqueous solutions. The linear relation between thickness and color signal can be lost once this layer forms on the copper surface of the calibration samples. To minimize the effects of such layers, we pre-etch all our copper films in a pH 3 hydrochloric acid solution for 5 s immediately before the optical measurement. This pre-etching is responsible for a shift of the curves displayed in Figs. 1(c) and 1(d). Since during the etching a small amount of material is removed, islands measured with the profiler to have a thickness of 5 nm or less were completely dissolved and consequently did not give rise to a color signal.

Based on our calibration measurements, we analyzed the dissolution of disk-shaped copper islands *in situ* using an experimental setup as shown in Fig. 2(a). Copper thin films were prepared as described above with a thickness of about 30 nm. Prior to each dissolution experiment, the thickness of each analyzed copper structure was measured with a profiler. Samples were pre-etched to avoid the presence of oxide layers. The dissolution of the copper island was initiated by adding a pH 3 hydrochloric acid solution to the copper-gold pair and covering the polydimethylsiloxane spacer with a cover glass (see Fig. 2). Images were recorded at a rate of 1 Hz and stored on a computer.

As in our calibration measurements, our time series is analyzed in MATLAB™ by calculating the color difference between the copper island and the gold surface for each image pixel. In order to reduce pixel noise, the color signal is averaged over 2×2 or 3×3 pixels depending on the desired noise reduction. We assign the thickness value of the as-prepared copper island (measured with the profiler prior to the experiment) to the color signal observed at the initial stage of the dissolution experiment. Based on the linear relation between the color signal and the copper film thickness [Fig. 1(d)], we obtain the thickness of the dissolving film by linear interpolation between the initial value of the color signal (corresponding to the initial thickness) and zero (no film present).

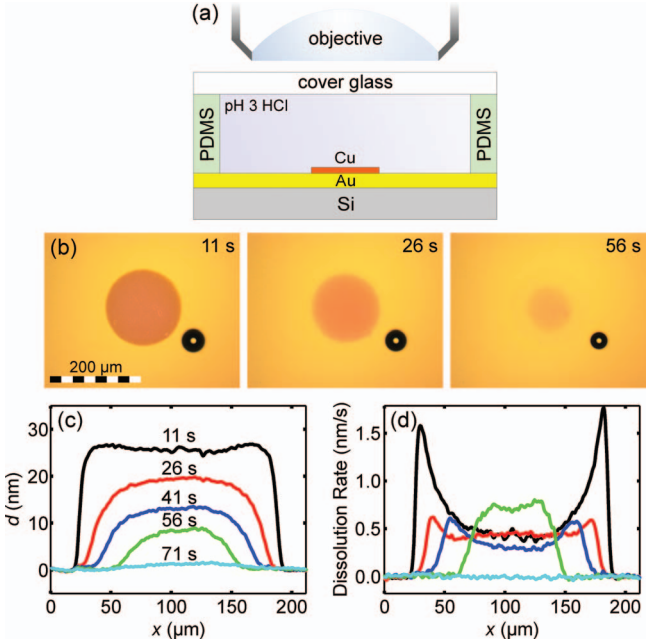

FIG. 2. *In situ* dissolution analysis. (a) Experimental setup. (b) Snapshots of a copper island dissolving in pH 3 hydrochloric acid at indicated times after initiation of the experiment. The small circular feature at the bottom right is an air bubble which became trapped inside the system. (c) Height profiles for indicated times corresponding to the measurement shown in (b). (c) Calculated dissolution rate (see text).

While the dissolution process takes place, the color difference slowly decreases until the whole image shows the color of the gold substrate [Fig. 2(b)]. Within less than 2 min the copper film is no longer visible in the optical image and the calculated film thickness is zero as can be seen in the cross sections displayed in Fig. 2(c). The dissolution process proceeds in a nonuniform fashion. While the edges of the copper island react away within the first 20 s, it takes more than 70 s until the center of the island is dissolved.

This is more easily visible when we calculate the time derivative of the film thickness, d, at every image pixel. We define a dissolution rate r as

$$r(\vec{x},t) = -\frac{\partial d(\vec{x},t)}{\partial t}. \quad (1)$$

In Fig. 2(d), the dissolution rate is plotted along a linear cross section through the copper island. As can be seen in Fig. 2, the dissolution rate is initially high at the edges of the island reaching values up to 1.5 nm/s. In the center, the dissolution rate is comparably low with a minimum of about 0.5 nm/s. As the dissolution reaction proceeds, the spatial distribution of the dissolution rate becomes more uniform and increases in the center of the copper island. Toward the end of the reaction, the dissolution rate in the center reaches a maximum of about 0.7 nm/s.

In order to compare our data more easily with other spatially resolved techniques, we estimate an electric current density corresponding to the measured dissolution rate. For this purpose, we assume that the dissolution of copper in a

pH 3 hydrochloric acid solution proceeds electrochemically according to the following simplified reaction scheme:[27]

$$\mathrm{Cu} + 2\mathrm{Cl}^- \rightleftharpoons \mathrm{CuCl}^-_{2,\mathrm{ads}} + e^-,$$
$$\mathrm{CuCl}^-_{2,\mathrm{ads}} + \mathrm{H_2O} \rightleftharpoons \mathrm{Cu_2O_{ads}} + 2\mathrm{H}^+ + 4\mathrm{Cl}^-. \quad (2)$$

Thus, we assume that the oxidation of copper in our system proceeds as a one-electron process. Based on the bulk density of copper and its molar mass, we can obtain an estimate for the local current density i from the dissolution rate r in the following way:

$$i(\vec{x},t) = r(\vec{x},t)\rho_{\mathrm{Cu}} M^{-1}_{\mathrm{Cu}} N_{\mathrm{A}} e. \quad (3)$$

Here, ρ_{Cu} and M_{Cu} denote the density and molar mass of copper, respectively, N_{A} is Avogadro's constant, and e is the elementary charge. Since we did not prove that the density of an electrolessly plated copper thin film is the same as for bulk copper, our calculation at this point contains a systematic error. Additionally, also non-Faradaic processes could potentially contribute to a dissolution process. However, the order of magnitude and relative distribution of current density can be determined. A dissolution rate of 1 nm/s corresponds to a current density of about 1.4 $\mathrm{mA/cm^2}$.

This calculation demonstrates that the sensitivity for copper dissolution depends on the time resolution. Height data calculated from one single image of the copper island are significantly affected by noise from the CCD camera. By averaging over a sufficiently large number of image frames, this noise can be substantially reduced. Over time intervals of several minutes, a color change corresponding to a decrease in thickness of 1 nm can be detected this way. The corresponding dissolution rate of the order of 1 nm/min is equivalent to a current density of about 20 $\mu\mathrm{A/cm^2}$. By integrating the current density over the total surface of the copper island, we estimate the total corrosion current. For a copper island with a diameter of 130 μm and an average current density of 20 $\mu\mathrm{A/cm^2}$, this results in a total current of 2.7 nA. If only a part of the copper disk experiences the smallest detectable current density or if a smaller copper structure was employed in the experiment, the minimum total dissolution current would scale accordingly.

The sensitivity of our reflectance technique can compete with other optical methods that have been employed for the measurement of dissolution or deposition rates. IE, which can be considered the most sensitive optical technique, is principally capable of detecting submonolayer changes in film thickness. When used *in situ*, however, the technique can be compromised by polarization effects within the electrochemical system, such as concentration gradients.[16,17] Phase-shifting IM, which is presumably less affected by electrolyte-induced artifacts, reaches a resolution in terms of film thickness on the order of 1 nm,[21,22] but it requires complicated instrumentation and offers only limited spatiotemporal resolution. As mentioned in the introduction, nonoptical methods such as *in situ* STM[10–13] achieve atomic resolution but at the cost of reduced temporal resolution. Eventually, the specific application determines whether our simple reflectance technique will be sufficient or whether a more sophisticated approach is necessary.

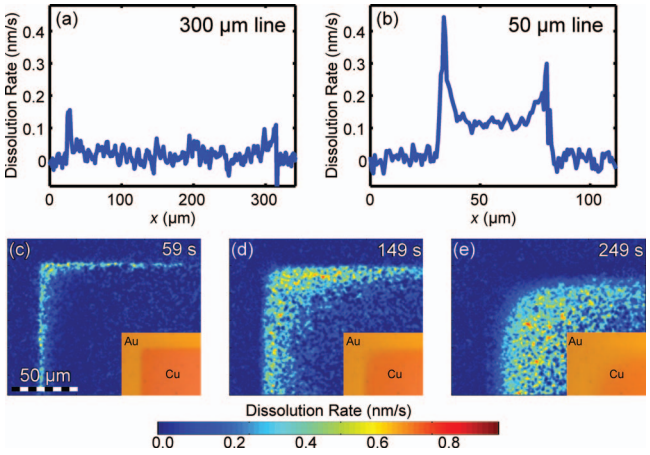

FIG. 3. Geometry-dependent dissolution behavior. [(a) and (b)] Dissolution rates for copper lines of different width (cross sections). [(c)–(e)] Two-dimensional map of the dissolution rate at the corner of a Cu electrode at indicated time moments. The dissolution rate is at a maximum at the corner of the Cu structure. Insets show the corresponding optical bright field images of the copper electrode on a smaller scale.

In the following, we illustrate the capabilities of our method by analyzing the dissolution rate distribution in different electrode configurations. Depending on electrode geometry and size, the dissolution dynamics of copper islands on gold in a pH 3 hydrochloric acid solution vary strongly. This is illustrated in Figs. 3(a) and 3(b), where we show the dissolution of single copper lines of different width. While a line with a width of 300 μm shows an initial maximum dissolution rate of about 0.1 nm/s at the copper-gold interface, a line with 50 μm width experiences a dissolution rate of up to 0.4 nm/s.

Not only the size but also the shape of the dissolving copper electrodes has an impact on the dissolution dynamics and its variation in time. This is illustrated in Figs. 3(c)–3(e), where we show the dissolution rate at the end of a copper line. Similar to what we have seen before, the dissolution reaction is initially strongly localized. Additionally, we observe that the dissolution rate is larger at the corner of the line structure than at the edges. As the reaction proceeds and the area of the copper electrode experiencing significant dissolution increases, the dissolution rate at the corner of the electrode stays larger than the dissolution rate along the edges. This observation can be further supported by the data shown in Fig. 2. Compared to the dissolution rate of up to 1.5 nm/s observed with circular copper islands (Fig. 2), the dissolution of both the narrow and the wide line shown in Figs. 3(a) and 3(b) proceeds slowly.

These observations illustrate that our method provides a simple way to systematically analyze the factors determining current distribution in electrochemical systems. In a slightly modified setup, where, for example, the contact resistance between the copper anode and the gold cathode can be externally controlled, we can try to determine whether observed current heterogeneities are simply caused by geometric effects and the corresponding Ohmic drops in the electrolyte (primary current distribution)[28] or by polarization effects due to concentration overpotential (tertiary current distribution).

In our specific system—galvanic oxidation of copper in mild hydrochloric acid in a coplanar electrode geometry—primary effects are likely to cause the observed heterogeneities, since at the copper-gold interface the Ohmic drop in the electrolyte is drastically reduced compared to an area at the center of the copper anode. However, the estimated current densities of several mA/cm^2 indicate that both reaction overpotentials and concentration overpotentials might play an important role, too. Therefore, we believe that the observed heterogeneities in dissolution rate have their origin in a complicated interplay between Ohmic potential drops as well as kinetic and ion-transport-induced limitations. A more detailed analysis of the dissolution dynamics will be the topic of a future publication.

IV. CONCLUSIONS

The gradual change in transmission and reflection properties as observed for copper thin films on gold is a universal property of all thin films with significant absorbance. Therefore, the computer-aided calibration of color data with respect to film thickness can be performed for a variety of materials including metal thin films, passive films, semiconductors, or polymers. Films can be observed on arbitrary, not necessarily conductive, flat substrates. Furthermore, as with every optical method, the detection of material dissolution or deposition is not restricted to Faradaic corrosion processes. Thus, our method of analysis based on optical bright-field imaging can be a versatile approach for the detection of any change in thin film properties, such as thickness, composition, or porosity that cause changes in the film's optical properties, and can be applied not only for thin film dissolution but in particular also for monitoring film deposition *in situ*. The measurement takes place in a noninvasive fashion and does not require any electrical or other physical contacts between the dissolving or corroding film and the measurement device. The technique provides a high spatial and temporal resolution, can be combined with standard electrochemical methods, and is sufficiently sensitive to measure dissolution rates on the order of a few nm/min.

So far, we employed our method for the measurement of corrosion inhibition using surfactants as corrosion inhibitors, and for the quantitative analysis of current distributions in galvanic microreactors used for the guided aggregation of colloidal particles. Due to its simplicity, our approach should be applicable to a variety of other experimental systems ranging from thin-film sensors[29] to insulating coatings.[30] Our method is not restricted to thin film monitoring in an electrochemical environment but can be applied in any optically transparent medium.

ACKNOWLEDGMENTS

The authors wish to thank Boris Khusid for stimulating discussions. This work was supported by ARO/MURI Grant Nos. W911NF-04-1-0170 and W911F-09-1-0476, and NASA University Research, Engineering, and Technology Institute on BioInspired Materials (BIMat) under Award No. NCC-1-02037. C.P. also acknowledges financial support from the Alexander von Humboldt Foundation.

[1] H. Kahn, C. Deeb, I. Chasiotis, and A. H. Heuer, J. Microelectromech. Syst. **14**, 914 (2005).
[2] D. C. Miller, W. L. Hughes, Z. L. Wang, K. Gall, and C. R. Stoldt, J. Microelectromech. Syst. **16**, 87 (2007).
[3] O. N. Pierron, D. D. Macdonald, and C. L. Muhlstein, Appl. Phys. Lett. **86**, 211919 (2005).
[4] C. Blanc, A. Freulon, M. C. Lafont, Y. Kihn, and G. Mankowski, Corros. Sci. **48**, 3838 (2006).
[5] R. H. Jones, D. R. Baer, M. J. Danielson, and J. S. Vetrano, Metall. Mater. Trans. A **32**, 1699 (2001).
[6] J. B. Jorcin, C. Blanc, N. Pebere, B. Tribollet, and V. Vivier, J. Electrochem. Soc. **155**, C46 (2008).
[7] K. A. Yasakau, M. L. Zheludkevich, S. V. Lamaka, and M. G. S. Ferreira, Electrochim. Acta **52**, 7651 (2007).
[8] A. J. Bard, F. R. F. Fan, D. T. Pierce, P. R. Unwin, D. O. Wipf, and F. M. Zhou, Science **254**, 68 (1991).
[9] A. J. Bard, F. R. F. Fan, J. Kwak, and O. Lev, Anal. Chem. **61**, 132 (1989).
[10] M. R. Vogt, A. Lachenwitzer, O. M. Magnussen, and R. J. Behm, Surf. Sci. **399**, 49 (1998).
[11] F. A. Möller, J. Kintrup, A. Lachenwitzer, O. M. Magnussen, and R. J. Behm, Phys. Rev. B **56**, 12506 (1997).
[12] H. Böhni, T. Suter, and A. Schreyer, Electrochim. Acta **40**, 1361 (1995).
[13] D. W. Suggs and A. J. Bard, J. Am. Chem. Soc. **116**, 10725 (1994).
[14] L. Lacroix, L. Ressier, C. Blanc, and G. Mankowski, J. Electrochem. Soc. **155**, C131 (2008).
[15] P. Schmutz and G. S. Frankel, J. Electrochem. Soc. **145**, 2295 (1998).
[16] M. Dornhege, C. Punckt, J. L. Hudson, and H. H. Rotermund, J. Electrochem. Soc. **154**, C24 (2007).
[17] C. Punckt, M. Bölscher, H. H. Rotermund, A. S. Mikhailov, L. Organ, N. Budiansky, J. R. Scully, and J. L. Hudson, Science **305**, 1133 (2004).
[18] A. Michaelis and J. W. Schultze, Phys. Chem. Chem. Phys. **97**, 431 (1993).
[19] C. C. Streinz, J. W. Wagner, J. Kruger, and P. J. Moran, J. Electrochem. Soc. **139**, 711 (1992).
[20] K. Habib, F. Al-Sabti, and H. Al-Mazeedi, Opt. Lasers Eng. **27**, 227 (1997).
[21] C. Blanc, Y. Roques, and G. Mankowski, Corros. Sci. **40**, 1019 (1998).
[22] Q. J. Chi, T. Tatsuma, M. Ozaki, T. Sotomura, and N. Oyama, J. Electrochem. Soc. **145**, 2369 (1998).
[23] G. O. Ilevbare, O. Schneider, R. G. Kelly, and J. R. Scully, J. Electrochem. Soc. **151**, B453 (2004).
[24] M. Büchler, P. Schmuki, and H. Böhni, J. Electrochem. Soc. **144**, 2307 (1997).
[25] C. M. Murira, C. Punckt, H. C. Schniepp, B. Khusid, and I. A. Aksay, Langmuir **24**, 14269 (2008).
[26] M. Born and E. Wolf, *Principles of Optics*, 7th ed. (Cambridge University Press, Cambridge, 2005).
[27] G. Bech-Nielsen, M. Jaskula, I. Chorkendorff, and J. Larsen, Electrochim. Acta **47**, 4279 (2002).
[28] N. Ibl, in *Comprehensive Treatise of Electrochemistry*, edited by E. Yeager, J. O. M. Bockris, B. E. Conway, and S. Sarangapani (Plenum, New York, 1983), Vol. 6.
[29] Y. Zhou, S. Jiang, S. Krause, and J. N. Chazalviel, Anal. Chem. **79**, 8974 (2007).
[30] S. Katayama, N. Akao, N. Hara, and K. Sugimoto, J. Electrochem. Soc. **152**, B286 (2005).